PLAGIOCLASE-FACIES THERMOBAROMETRIC EVOLUTION OF THE EXTERNAL LIGURIDE PYROXENITE-BEARING MANTLE (SUVERO, ITALY)

Valentin Basch*,✉, Giulio Borghini, Patrizia Fumagalli**, Elisabetta Rampone*,✉, Andrea Gandolfo*** and **Carlotta Ferrando*****

* *Dipartimento di Scienze della Terra, dell'Ambiente e della Vita, University of Genova, Italy.*
** *Dipartimento di Scienze della Terra "Ardito Desio", University of Milano, Italy.*
*** *CRPG, University of Lorraine, Nancy, France.*
✉ *Corresponding authors: Rampone, email: elisabetta.rampone@unige.it; Basch, email: valentin.basch@gmail.com*

Keywords: *pyroxenites; plagioclase peridotite; veined mantle exhumation; geobarometer; extending lithosphere; Suvero; Northern Apennines; Italy.*

ABSTRACT

Plagioclase peridotites are an important marker of the shallow geodynamic evolution of the lithospheric mantle at extensional settings. Based on low-pressure experiments, a recent study by Fumagalli et al. (2017) defined and calibrated a geobarometer for peridotitic bulk compositions, based on the Forsterite-Anorthite-Ca-Tschermak-Enstatite (FACE) pressure-sensitive equilibrium. The Suvero plagioclase-bearing peridotites, on which the FACE geobarometer was calibrated, are primarily associated to plagioclase pyroxenites. Assuming that the pyroxenites record the same Pressure-Temperature evolution than the plagioclase peridotites, they represent ideal candidates to test the applicability of the FACE geobarometer on pyroxenitic compositions. As documented in the plagioclase peridotites, the pyroxenites are characterized by the development of fine-grained neoblastic assemblages, indicative of partial recrystallization under plagioclase-facies conditions. Chemical zonations in these neoblastic mineral aggregates suggest equilibration stages at variable pressure and temperature and allowed to document two re-equilibration stages corresponding to the onset of plagioclase-facies recrystallization (830-850°C, 6.9-8.1±0.5 kbar) and a shallower colder re-equilibration (770-790°C, 5.8-5.9±0.5 kbar), respectively. The decompressional evolution reported for pyroxenitic bulk compositions is consistent with the exhumation history documented in the associated Suvero peridotite, although at slightly higher equilibrium pressures (~ 1 kbar). Remarkably, the much lower X_{Cr} in pyroxenites reflects in lower Cr incorporation in pyroxenes and, consequently, in significantly higher Ca-Tschermak activity in clinopyroxene that might introduce the systematic pressure overestimation by FACE geobarometer.

INTRODUCTION

Plagioclase peridotites are extensively described in slow to ultraslow-spreading ridges and passive margins (e.g., Kelemen et al., 2007; Dick et al., 2010; Martin et al., 2014; Warren, 2016; Basch et al., 2018), where extension is dominated by tectonic denudation and mantle is exhumed by kilometre-scale detachment faults (e.g., Piccardo et al., 1993; 2002; Rampone and Piccardo, 2000; Manatschal and Müntener, 2009; MacLeod et al., 2009). The formation of plagioclase in these mantle rocks can be related either to magmatic crystallization during percolation of tholeiitic melts within the peridotites or metamorphic recrystallization at plagioclase-facies conditions. The two processes imply a different thermal structure of the lithosphere and can affect different mantle sections of an extending lithosphere, i.e. hot, infiltrated mantle domains affected by melt percolation and melt-rock interaction during exhumation, or cold mantle sectors which were exhumed at subsolidus conditions, thus recording low-pressure metamorphic recrystallization (Rampone et al., 2018). In both cases, plagioclase peridotites constitute an important marker of the shallow geodynamic evolution of the lithospheric mantle at extensional settings.

Experiments on fertile and depleted peridotites within the subsolidus plagioclase stability field (Borghini et al., 2010) demonstrated that the compositions of coexisting plagioclase and pyroxenes are not dependent on the peridotite bulk composition and vary significantly over a rather narrow pressure range. Borghini et al. (2011) proposed an empirical geobarometer based on the composition of plagioclase and applied it on chemically zoned plagioclase-bearing neoblastic aggregates in the Suvero plagioclase peridotites (External Liguride Unit, Northern Apennines, Italy), obtaining pressure estimates from 7 to 3 kbar (i.e. ~ 21 to 9 km; Borghini et al., 2011). More recently, Fumagalli et al. (2017) further investigated experimentally the variability of mineral chemistry in a Na-rich peridotite within the plagioclase-facies. Profiting of a consistent experimental database, covering a wide range of P-T conditions (3-9 kbar, 1000-1150°C) and variable bulk compositions, they calibrated a geobarometer for plagioclase peridotites based on the reaction $Forsterite^{Ol} + Anorthite^{Pl} = Ca\text{-}Tschermak^{Cpx} + Enstatite^{Opx}$ (FACE geobarometer, Fumagalli et al., 2017). The application of the FACE geobarometer, adequately supported by detailed microstructural and mineral chemistry investigations, provides a valuable tool to track the exhumation of the lithospheric mantle in extensional environments.

The Suvero ultramafic body is heterogeneous and characterized by the occurrence of parallel spinel pyroxenite layers within spinel lherzolites (Borghini et al., 2011; 2013; 2016; 2019). These pyroxenite layers were interpreted as the result of old (Ordovician; 433±51 Ma; Borghini et al., 2013) high-pressure segregation (P > 15 kbar) and reactive crystallization of low-MgO silica-saturated melts likely originated by melting of a heterogeneous mantle source (Borghini et al., 2016). Host peridotites and pyroxenite layers were already associated prior to the Jurassic exhumation of this subcontinental mantle sector and presumably experienced the same decompressional Pressure-Temperature evolution leading to partial recrystallization at plagioclase-

facies conditions. Pyroxenite layers are characterized by rather fertile bulk compositions and are, therefore, more sensible to plagioclase-facies recrystallization (Hidas et al., 2013; Fumagalli et al., 2017; Borghini and Fumagalli, 2018). Subsolidus phase relations have been experimentally defined for a pyroxenite sample (GV10) from the Suvero massif (Borghini and Fumagalli, 2018). Few experiments on pyroxenite GV10 at plagioclase-facies conditions have provided plagioclase composition comparable with those observed in the host peridotite, but more experimental data on plagioclase-bearing pyroxenites are needed to extend the applicability of the FACE geobarometer to pyroxenitic compositions. The more fertile character of pyroxenites with respect to peridotites enhances subsolidus recrystallization processes (Hidas et al., 2013; Borghini et al., 2016; Borghini and Fumagalli, 2018) and can therefore facilitate the geobarometric estimates for pyroxenite-bearing mantle sectors. Moreover, fertile pyroxenites are expected to encounter plagioclase appearance at significantly higher pressure than peridotite (Borghini and Fumagalli, 2018) and thus they are potentially good markers of low-pressure equilibration of the mantle rocks.

In this article, we present a detailed microstructural-based chemical work on the neoblastic plagioclase-facies mineral assemblage on selected pyroxenite samples. The main objectives of this paper are to: *i)* document the low-pressure evolution as recorded by pyroxenite layers that are directly associated to plagioclase peridotites previously investigated (Borghini et al., 2011); and *ii)* test the applicability of the FACE geobarometer on pyroxenitic compositions.

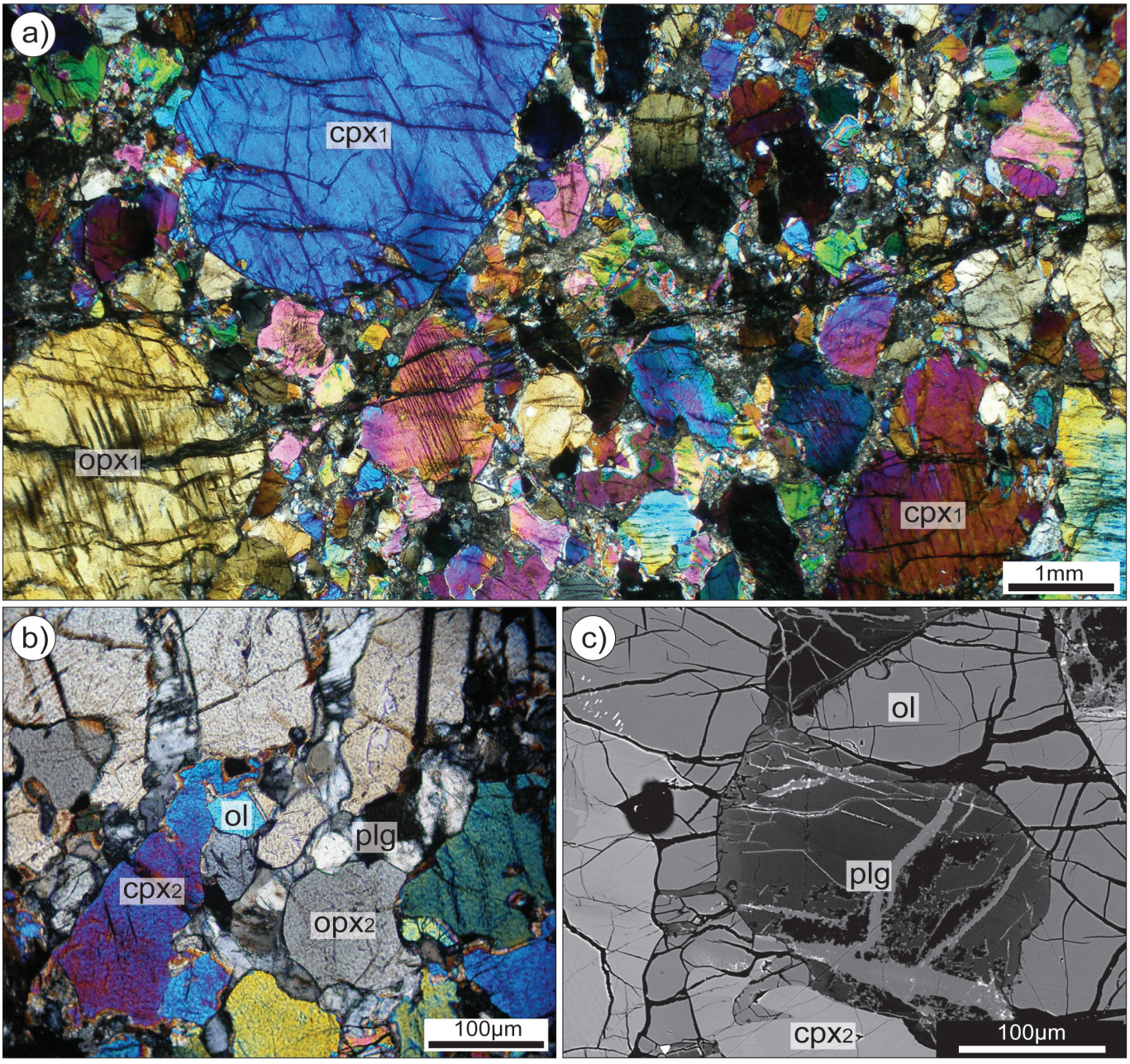

Fig. 1 - Photomicrographs and BSE image of representative textures observed in the Suvero plagioclase-bearing pyroxenites. a) Partially recrystallized spinel-facies porphyroclastic assemblage; b) Detail of the plagioclase-bearing neoblastic assemblage; c) BSE image of the plagioclase-bearing neoblastic assemblage. The colour variation within plagioclase is indicative of a core-rim chemical zoning. cpx- clinopyroxene; opx- orthopyroxene; plg- plagioclase; ol- olivine.

PETROLOGICAL BACKGROUND AND SAMPLES

The Alpine-Apennine ophiolites represent lithospheric remnants of the Ligurian Tethys Ocean (e.g., Rampone et al., 2018 and references therein). Jurassic opening of the oceanic basin led to a progressive uplift and exhumation of subcontinental lithospheric mantle (e.g., Manatschal and Müntener, 2009). Most of these mantle bodies have been affected by refertilization processes related to the asthenospheric upwelling during rifting and subsequent oceanization (e.g., Rampone et al., 1997; 2004; 2008; 2016; 2018, Müntener et al., 2004; Borghini et al., 2007; Piccardo et al., 2002; 2007; Basch et al., 2018; 2019a; 2019b). However, some mantle units from the Northern Apennines (including the External Liguride Unit) have escaped this melt-rock interaction history and preserve their pristine subcontinental lithospheric mantle composition (Beccaluva et al., 1984; Rampone et al., 1995; Montanini et al., 2006; Borghini et al., 2011; 2016).

The External Liguride (EL) ophiolites are composed of kilometre-scale bodies of ultramafic rocks and minor MORB-type gabbros and basalts, embedded in Cretaceous sedimentary mélanges that were obducted during closure of the Ligurian Tethys oceanic basin (Rampone et al., 1993; 1995; Tribuzio et al., 2004; Montanini et al. 2008). The External Liguride ophiolitic mantle sequences have therefore been inferred to represent remnants of a fossil ocean-continent transition, where exhumed subcontinental mantle was associated with embryonic oceanic crust and rocks of continental origin (Marroni et al., 1998; Rampone and Piccardo, 2000; Tribuzio et al., 2004; Montanini et al., 2008). The mantle sequences consist of fertile spinel and plagioclase lherzolites with disseminated Ti-rich amphibole and widespread spinel- or garnet-bearing pyroxenite layers (Beccaluva et al., 1984; Rampone et al., 1993; 1995; Montanini et al., 2006; 2012; Borghini et al., 2013; 2016; Montanini and Tribuzio, 2015).

In the Suvero peridotites, the development of fine-grained plagioclase-bearing neoblastic aggregates is indicative of partial metamorphic recrystallization of the spinel-facies porphyroclastic mineral assemblage (Rampone et al., 1993; 1995; Borghini et al., 2011). This recrystallization witnesses the decompressional evolution of the peridotites from spinel-facies (1.2-1.5 GPa, 950-1000°C) to plagioclase-facies conditions (< 1 GPa, 800-900°C; Borghini et al., 2011). Moreover, compositional zoning in neoblasts (e.g., anorthite content reverse zoning; An = Ca/(Ca + Na) mol%) resulted from subsolidus decompressional evolution of the peridotites within plagioclase-facies stability field. In the peridotites, detailed microstructural-geochemical analyses (Borghini et al., 2011) combined with the application of the FACE geobarometer (Fumagalli et al., 2017), allowed to estimate two stages of recrystallization, from 6.3-7.0 kbar at 840-900°C to 4.3-4.8 kbar at 800-850°C (Fumagalli et al. 2017).

At Suvero, peridotites are associated to spinel-bearing pyroxenite occurring as parallel layers within the lherzolites and ranging in thickness from millimetre- to decimetre-scale. Pyroxenite layers are parallel to the mantle tectonite foliation plane and show sharp contacts with the host peridotites characterized by occurrence of thin irregular orthopyroxene-rich borders along pyroxenite-peridotite contact (Borghini et al., 2019). Pyroxenite abundance is variable and can be as high as 50% in some outcrops (see Fig. 2 in Borghini et al., 2016). In some places, pyroxenite layers alternate with harzburgite and dunite, forming compositional layering parallel to the tectonite.

Pyroxenites consist of a primary spinel-bearing mineral association made by coarse-grained clinopyroxene, orthopyroxene and spinel (up to centimetre-size crystals; Fig. 1a), elongated along the mantle foliation observed in the peridotites. The porphyroclastic minerals are partially recrystallized, indicating low-pressure metamorphic reequilibration during decompression from spinel- to plagioclase-facies conditions (Borghini et al., 2016). This recrystallization is marked by the development of: *i)* sub-millimetre to millimetre-size coronas of plagioclase and olivine around coarse porphyroclasts of greenish spinel; *ii)* orthopyroxene and plagioclase exsolution in porphyroclastic clinopyroxenes; and *iii)* fine-grained neoblastic aggregates (~ 100-200 μm) of pyroxenes, plagioclase and olivine partially replacing the spinel-facies pyroxene porphyroclasts (Fig. 1b, c).

In order to study the plagioclase-facies geothermobarometric evolution recorded in the pyroxenite layers, we selected three pyroxenite samples previously investigated by Borghini et al. (2016). They are two websterites (GV8 and GV10) and a clinopyroxene-rich websterite (BG13) and preserve unaltered neoblastic aggregates of clinopyroxene$_2$ + orthopyroxene$_2$ + plagioclase + olivine. These samples exhibit more fertile bulk compositions than the host peridotites i.e. they are characterized by lower Mg-values (82.53-84.98 mol%), higher CaO (12.6-14.0 wt%), Al_2O_3 (9.9-13.8 wt%) and Na_2O (0.4-0.5 wt%) (Table 1, Fig. 2). The Na_2O/CaO and Cr/(Cr + Al) ratios of the pyroxenite samples (Na_2O/CaO = 0.032-0.041; Cr/(Cr + Al) = 0.007-0.011 mol%) also plot far from the compositional range defined by the host plagioclase peridotites (Fig. 3). Moreover, the pyroxenite GV10 has been selected as starting bulk composition for partial melting and subsolidus experiments at 7-15 kbar (Borghini et al., 2017; Borghini and Fumagalli, 2018).

ANALYTICAL METHODS

Major element (SiO_2, TiO_2, Al_2O_3, Cr_2O_3, FeO, MgO, MnO, CaO, NiO and Na_2O) compositions of olivine, clinopyroxene, orthopyroxene and plagioclase were analyzed by JEOL JXA 8200 Superprobe equipped with five

Table 1 - Bulk rock major element compositions of the plagioclase pyroxenite, after Borghini et al. (2016).

wt%	BG13	GV8	GV10
SiO_2	43.84	46.46	45.99
TiO_2	0.42	0.45	0.44
Cr_2O_3	0.14	0.17	0.16
Al_2O_3	13.83	11.5	9.94
FeOt	6.55	6.71	7.77
MnO	0.19	0.14	0.16
MgO	18.06	19.17	18.53
CaO	13.33	12.64	13.96
Na_2O	0.42	0.52	0.48
LOI	4.48	3.13	2.82
Total	101.26	100.89	100.25
Mg#	84.52	84.98	82.53
Na_2O/CaO	0.032	0.041	0.034
Cr/(Cr+Al)	0.007	0.010	0.011

Mg# = Mg/(Mg + Fe).

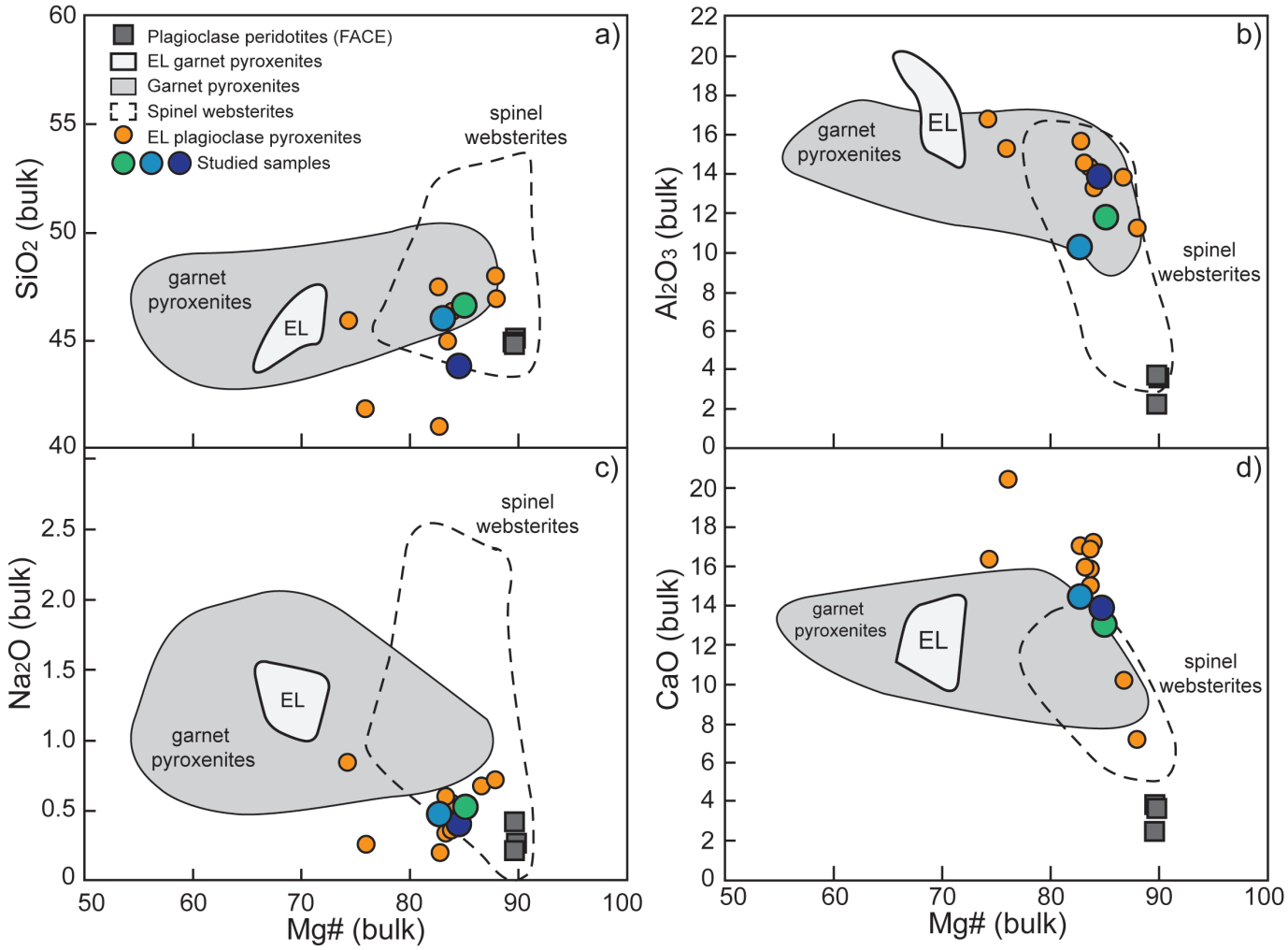

Fig. 2 - Variation diagrams of Mg# vs a) SiO_2, b) Al_2O_3, c) Na_2O, d) CaO (wt%) for the External Ligurides (EL) plagioclase pyroxenites (Borghini et al., 2016) and studied samples. Compositional fields are garnet pyroxenites and spinel websterites from ultramafic orogenic massifs: Beni Bousera, Morocco (Pearson et al., 1993; Kumar et al., 1996; Gysi et al., 2011); Ronda, Spain (Suen and Frey, 1987; Garrido and Bodinier, 1999; Bodinier et al., 2008); Horoman, Japan (Takazawa et al., 1999; Morishita and Arai, 2001); Pyrénées, France (Bodinier et al., 1987a; 1987b); Balmuccia, Italy (Sinigoi et al., 1983; Voshage et al., 1988; Mukasa and Shervais, 1999). The EL field refers to the bulk compositions of garnet pyroxenites of the External Liguride Units investigated by Montanini et al. (2006), and the grey squares represent the bulk composition of the Suvero plagioclase peridotites used by Fumagalli et al. (2017) to calibrate the FACE geobarometer. Mg# = Mg/(Mg+Fe) x 100.

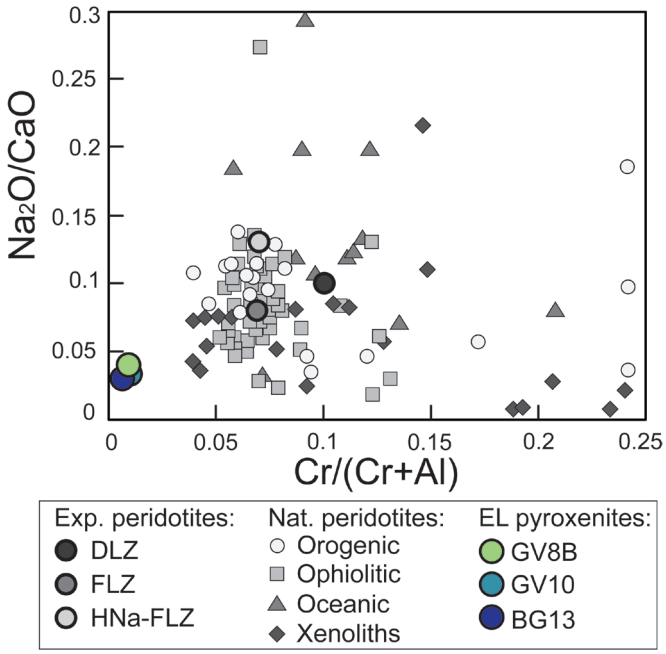

Fig. 3 - Cr/(Cr + Al) vs. Na_2O/CaO diagram comparing the External Ligurides pyroxenite bulk compositions (Table 1) to the composition of starting materials used in experimental studies. *FLZ* fertile lherzolite (Borghini et al., 2010; 2011; Fumagalli et al., 2017), *DLZ* depleted lherzolite (Borghini et al., 2010; Fumagalli et al., 2017) and *HNa-FLZ* high-Na fertile lherzolite (HNa-FLZ, Fumagalli et al., 2017) bulk compositions have been used to calibrate the FACE geobarometer (Fumagalli et al., 2017). Experimental starting materials are compared with the compositions of ophiolitic, orogenic and oceanic peridotites (Sinigoi et al., 1980; Bodinier et al., 1988; 2008; Voshage et al., 1988; Piccardo et al., 1988; Frey et al., 1991; Van der Wal and Vissers, 1996; Rampone et al., 1995; 1996; 2005; 2008; Takazawa et al., 2000; Niu 2004; Sano and Kimura, 2007; Le Roux et al., 2007; Kaczmarek and Müntener, 2010), and mantle xenoliths (Ionov et al., 1995; Bonadiman et al., 2005; Martin et al., 2014).

wavelength-dispersive spectrometers, an energy dispersive spectrometer, and a cathodoluminescence detector (accelerating potential 15 kV, beam current 15nA), operating at the Dipartimento di Scienze della Terra, University of Milano. Mineral chemistry of clinopyroxene, orthopyroxene, plagioclase and olivine from the studied pyroxenites are reported in Supplementary Tables 1S-4S. Our data are consistent with mineral compositions reported for these pyroxenite samples by Borghini et al. (2016).

MINERAL CHEMISTRY

Clinopyroxene, orthopyroxene and olivine show Mg-values consistent with their respective bulk-rock major element composition (Table 1). Within each sample, pyroxenes and olivine also show variations in Mg-value correlated to the mineral assemblage (porphyroclasts vs neoblasts) and microstructural site (core vs rim) they are found in.

Clinopyroxene (Table 1S) porphyroclasts show increasing Mg-values and decreasing Al_2O_3 contents from crystal cores (coloured circles; GV10: Mg# = 81.8-82.4 mol%, GV8 and BG13: Mg# = 83.7-84.0 mol%, Al_2O_3 = 7.8-8.4 wt%, Al a.p.f.u. = 0.32-0.37) to rims (open circles; BG13: Mg# = 85.2-87.5 mol%, Al_2O_3 = 3.7-5.7 wt%, Al a.p.f.u. = 0.16-0.25; Fig. 4a). They exhibit lower Cr_2O_3 contents (Cr_2O_3 = 0.10-0.35 wt%) than spinel-facies clinopyroxenes analyzed in the host peridotite (Borghini et al., 2011). Neoblastic clinopyroxenes (triangles in Fig. 4a) show higher Mg-values, lower Al_2O_3 and similar Cr_2O_3 contents relative to porphyroclasts, and increasing Mg-values at decreasing Al_2O_3 contents from crystal cores (GV10: Mg# = 81.2-82.0 mol%, GV8 and BG13: Mg# = 84.6-86.8 mol%, Al_2O_3 = 4.5-6.4 wt%, Al a.p.f.u. = 0.20-0.28, Cr_2O_3 = 0.09-0.39 wt%) to rims (GV10: Mg# = 81.3-82.0 mol%, GV8 and BG13: Mg# = 85.0-88.2 mol%, Al_2O_3 = 3.1-5.8 wt%, Al a.p.f.u. = 0.14-0.26, Cr_2O_3 = 0.13-0.39 wt%).

Orthopyroxene (Table 2S) porphyroclasts show increasing Mg-values at decreasing Al_2O_3 contents from crystal cores (GV10: Mg# = 81.5-82.3 mol%, GV8 and BG13: Mg# = 83.7-85.3 mol%, Al_2O_3 = 4.8-6.7 wt%, Al a.p.f.u. = 0.16-0.28) to rims (GV8: Mg# = 84.1-86.7 mol%, Al_2O_3 = 2.3-3.7 wt%, Al a.p.f.u. = 0.09-0.15; Fig. 4b). Porphyroclasts show similar CaO contents (CaO = 0.6-1.4 wt%) and lower Cr_2O_3 contents (Cr_2O_3 = 0.11-0.31 wt%) than spinel-facies orthopyroxenes analyzed in the host peridotite (Borghini et al., 2011). Granular orthopyroxenes (cores and rims) show similar Mg-values (GV10: Mg# = 81.1-81.5 mol%, GV8 and BG13 = 83.8-86.9 mol%), Al_2O_3 (Al_2O_3 = 2.0-3.9 wt%, Al a.p.f.u. = 0.09-0.15) and Cr_2O_3 contents (Cr_2O_3 = 0.04-0.21 wt%) to orthopyroxene porphyroclast rims (Fig. 4b).

Plagioclase (Table 3S) cores show rather homogeneous composition in all the analyzed samples. Anorthite content in plagioclase (An = Ca/(Ca + Na) × 100) varies from 56.2 to 62.4 mol%, and almost overlaps the anorthite variation observed in associated peridotite (An = 56-59 mol%, Borghini et al., 2011; Fig. 5). Rims of plagioclase crystals show variable compositions depending on which phase they are associated with. Rims at the contact with granular orthopyroxene and olivine show compositions similar to plagioclase cores (An = 55.5-59.2 mol%, Fig. 5). Some plagioclase rims at the contact with granular clinopyroxene show higher anorthite content (An = 74.3-76.6 mol%, Fig. 5), similar to the compositions of plagioclase rims in the host peridotites (An = 74-79 mol%, Borghini et al., 2011).

Olivine (Table 4S) cores in the different samples show rather homogeneous Forsterite contents that are positively correlated with their respective bulk-rock Mg-value (GV10: Fo = 80.5-81.7 mol%, GV8 and BG13: Fo = 86.1-86.9 mol%).

DISCUSSION

Thermobarometry of pyroxenites at plagioclase-facies conditions

The selected samples record the development of neoblastic aggregates (cpx_2 + opx_2 + plagioclase + olivine) at the expense of the primary spinel-facies porphyroclastic minerals, as a witness of partial plagioclase-facies recrystallization (Fig. 1). Core-to-rim chemical zonations in neoblastic mineral aggregates (Figs. 4, 5) suggest their re-equilibration at different stages of pressure and temperature (Borghini et al., 2011).

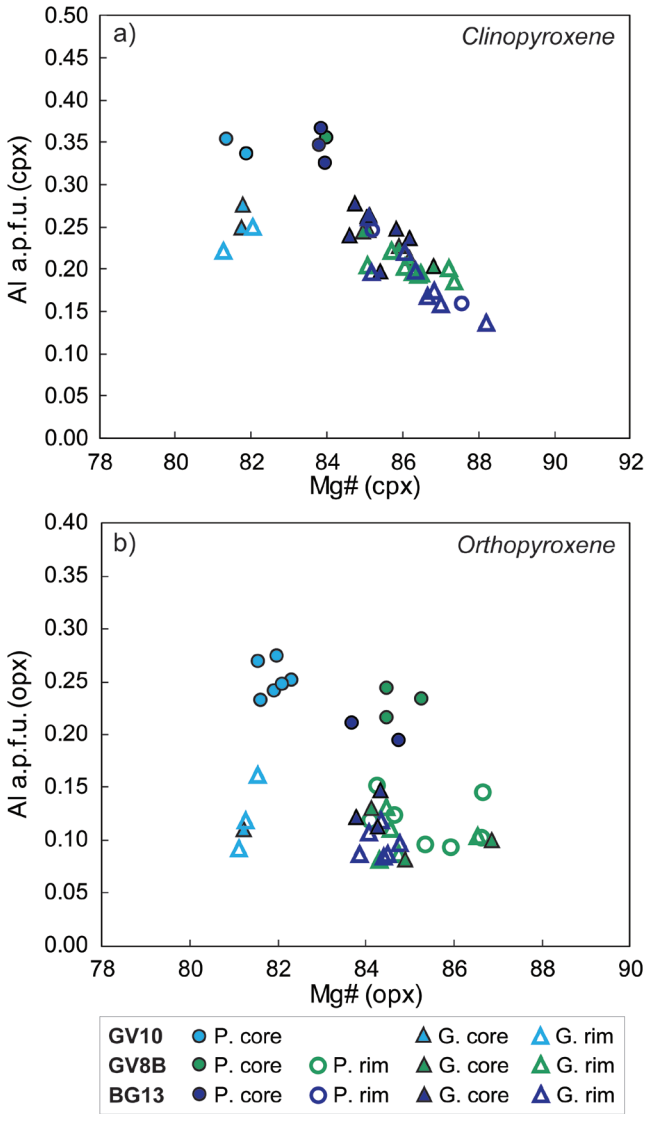

Fig. 4 - Variation of Mg# vs. Al content (a.p.f.u.) in clinopyroxenes (a) and orthopyroxenes (b) from the studied pyroxenites.

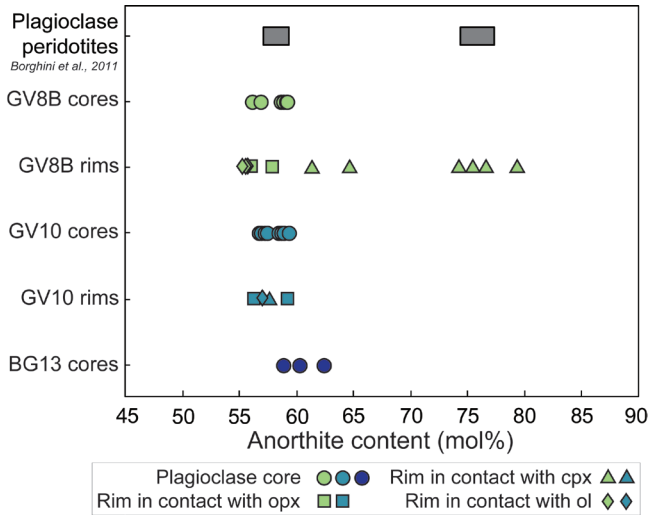

Fig. 5 - Variation in Anorthite content [An = Ca/(Ca+Na) x 100] between the different samples and the different microstructural sites. The grey squares report the compositions of plagioclase analyzed in the associated plagioclase peridotite (Borghini et al., 2011).

Following Borghini et al. (2011) approach on Suvero plagioclase peridotites, we focused on the most preserved plagioclase-bearing neoblastic assemblages in the studied pyroxenites. Careful microstructural observations combined with detailed mineral chemistry analysis allowed us to group the compositions of neoblasts cores, referring to an earlier recrystallization stage (Stage 1), and those of neoblastic rims, which record a shallower re-equilibration (Stage 2). The assumption that cores and rims of plagioclase and pyroxenes neoblasts are in chemical equilibrium is strongly supported by microstructural evidence indicating textural equilibrium (Fig. 3).

Element partitioning between texturally associated minerals has been used to test chemical equilibrium, mandatory for application of geothermobarometry. X_{Mg} in clinopyroxene, orthopyroxene and olivine cores and rims are coherent with Fe,Mg partitioning in ultramafic compositions (Table 1 and Table 1S, 2S, 4S). Plagioclase and clinopyroxene compositions further establish chemical equilibrium: anorthite in plagioclase vs. aluminium content in M1 of clinopyroxene (X_{Al}^{M1}; Fig. 6) follows the pressure-related trend observed in experiments (Fumagalli et al., 2017). Furthermore, Ca, Na partitioning between clinopyroxene and plagioclase (Fig. 6b) is strictly consistent with previous experimental and natural observations (Borghini et al., 2010; 2011; Fumagalli et al., 2017).

The geothermobarometric estimates obtained for the two equilibration conditions, Stage 1 and Stage 2, are reported in Table 2. Only the equilibrated mineral couples, i.e. respecting the documented Al_{M1}-An and Ca-Na element partitioning, were used for geothermobarometric calculations. We first estimated temperatures applying the two-pyroxene Fe-Mg geothermometer (Brey and Kohler, 1990; Taylor, 1998) and Ca-in-orthopyroxene geothermometer (Brey and Kohler, 1990). Overall, crystal cores yield equilibrium temperatures ($T_{Fe\text{-}Mg}$ ~ 830-850°C) higher than the crystal rims ($T_{Fe\text{-}Mg}$ ~ 770-790°C), consistently with the temperatures computed for the plagioclase-facies assemblages of the Suvero peridotites using the same geothermometers (Borghini et al., 2011; Fumagalli et al., 2017).

Pressure estimates were then obtained using the spreadsheet provided as supplementary material in Fumagalli et al. (2017) (Table 2). Cores record equilibrium pressures ranging from 6.9 to 8.1±0.5 kbar (Stage 1). According to the decompressional evolution recorded by plagioclase peridotites, the FACE estimates on the rims (Stage 2) give pressures of 5.8-5.9±0.5 kbar (Table 2). These two pressure intervals respectively represent the upper and lower pressure condition limits of the reequilibration stage in the plagioclase stability field. The core-rim zoning in neoblasts is likely the result of continuous chemical re-equilibration via solid-state element diffusion among plagioclase and pyroxenes during the decompressional evolution. In the peridotites, this has been well documented by progressive chemical variation along profiles on neoblasts (Borghini et al., 2011).

Plagioclase-facies evolution of the Suvero pyroxenite-peridotite association

FACE geobarometer applied to the Suvero plagioclase peridotites provided two stages of low-pressure re-crystallization at 6.3-7.0 and 4.3-4.8±0.5 kbar (Fumagalli et al., 2017). As the pyroxenites formation predates the exhumation of this mantle sector, we can assume that they experienced the same decompressional path. Indeed, thermobarometric estimates for pyroxenites (Table 2) indicate comparable pressure and temperature decrease (approx. 60°C, and 1.0-1.5 kbar) from the event recorded by neoblastic cores to the stage testified by rims. Nonetheless, pyroxenites yield slightly lower temperatures (ΔT ~ -30-40°C) and higher pressures (ΔP ~ 1 kbar) than neoblastic cores and rims in plagioclase peridotites.

Subsolidus experiments on mantle peridotites in complex chemical systems determined that the pressure of the plagioclase to spinel transition is strongly influenced by the

Table 2 - Geothermobarometric estimates based on major element compositions of the neoblastic minerals.

		Brey & Kohler (1990)		Taylor (1998)	Fumagalli et al. (2017)					
Sample	Assemblage	opx-cpx	Ca-in-opx	opx-cpx	aCaTs (cpx)	aEn	Xan (plg)	aFo	Kd (FACE)	P (kbar)
GV10	g. core	850	972	838	0.025	0.630	0.745	0.648	0.0327	7.5
GV10	g. core	809	972	789	0.031	0.630	0.723	0.648	0.0412	8.1
GV8B	g. core	806	922	768	0.025	0.725	0.738	0.756	0.0328	7.5
GV8B	g. core	938	887	926	0.017	0.687	0.942	0.756	0.0165	7.5
BG13	g. core	889	965	869	0.027	0.674	0.742	0.756	0.0327	6.9
BG13	g. core	828	962	814	0.017	0.685	1.003	0.756	0.0157	7.2
GV8B	rim-rim	772	883	747	0.022	0.677	0.781	0.744	0.0259	5.9
GV8B	rim-rim	801	907	786	0.025	0.668	0.770	0.744	0.0294	5.8

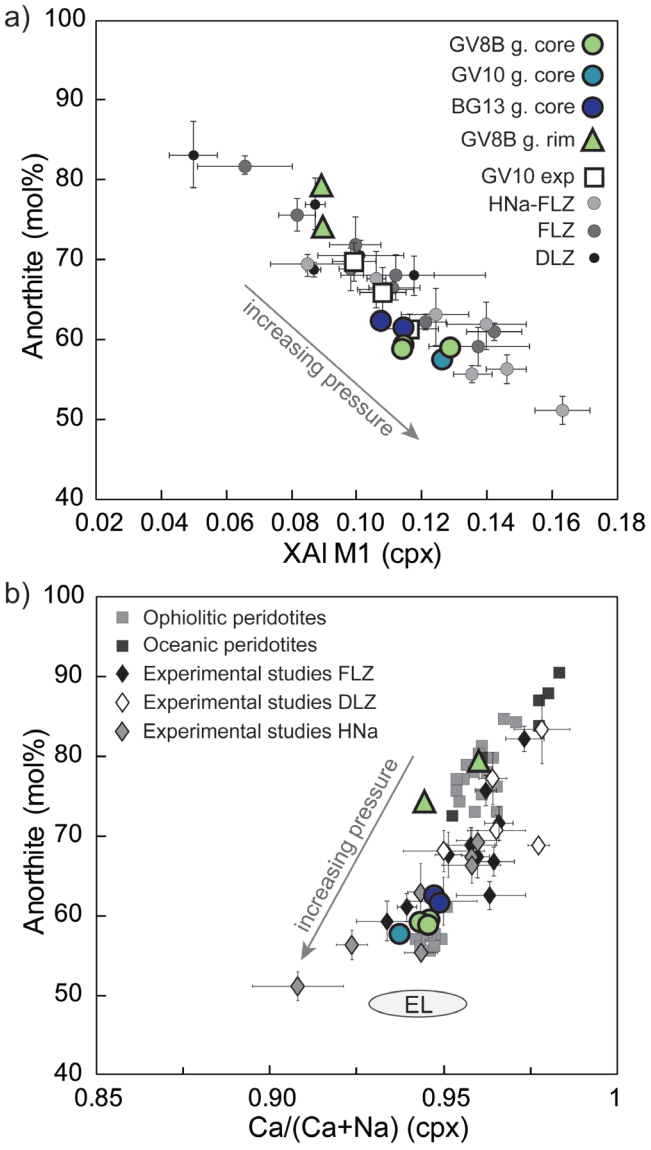

Fig. 6 - Diagrams showing the element partitioning between plagioclase and clinopyroxene from the selected mineral associations; a) pressure-dependent correlation between the XAl M1 in clinopyroxene and Anorthite content in plagioclase. Experimental data are from Fumagalli et al. (2017) and Borghini and Fumagalli et al. (2018); b) correlation between Ca/(C + Na) in clinopyroxene and Anorthite content in plagioclase. Data for comparison are from Borghini et al. (2010; 2011) and references therein.

combined effect of Na_2O/CaO (Ab/Di) and Cr/(Cr+Al) (X_{Cr}) ratios of the bulk composition (Green and Falloon, 1998; Borghini et al., 2010; Fumagalli et al., 2017). Increasing Ab/Di ratio favours the stability of plagioclase towards higher pressures, whereas an increase in X_{Cr} moves the plagioclase appearance to lower pressures (Borghini et al., 2010). Therefore, the plagioclase stability field is expected to progressively expand toward higher pressure from depleted peridotite to fertile peridotite and pyroxenite. Suvero pyroxenites have slightly lower Ab/Di (0.09-0.11) than the associated peridotites (Ab/Di = 0.15-0.16) and much lower bulk X_{Cr} (pyroxenites: X_{Cr} = 0.01; peridotites: X_{Cr} = 0.07). Accordingly, the transition from plagioclase to spinel facies for pyroxenite bulk compositions (GV10) has been experimentally located at 1 kbar higher than fertile peridotitic compositions, mostly due to its lower X_{Cr} (Fig. 2; Borghini and Fumagalli, 2018).

Fig. 7 displays the thermobarometric estimates obtained in the Suvero pyroxenites and peridotites at plagioclase-facies conditions (Fumagalli et al., 2017), compared to the experimentally determined plagioclase to spinel transition for their respective bulk composition (Fumagalli et al., 2017; Borghini and Fumagalli, 2018). The onset of plagioclase crystallization provided by the pressure estimate on the neoblastic cores (stage S1; Fig. 7) falls at the upper limit of the plagioclase-bearing field experimentally determined for the pyroxenite GV10 and the fertile lherzolite, respectively 8 kbar and 7 kbar at 850°C (Fig. 7). This result could indicate that pyroxenites record an initial stage of plagioclase-facies recrystallization at higher pressure than the associated peridotites in response to their more fertile bulk composition (i.e. much lower X_{Cr}). However, the shift towards higher pressure also obtained for Stage 2 (Fig. 7) suggests a slight systematic deviation when the FACE geobarometer is applied to pyroxenitic bulks. Indeed, FACE geobarometer was calibrated for mantle peridotites and a bulk composition effect on its pressure estimates on pyroxenites need to be further considered (Borghini and Fumagalli, 2018).

Bulk composition effect on FACE barometric estimates

As the Suvero peridotites and pyroxenites were exhumed together, they are expected to record the same, or rather similar, pressure and temperature conditions of the plagioclase-facies recrystallization stages (S1 and S2, Fig. 7). Although the onset of plagioclase-bearing crystallization may be anticipated to slightly higher depth in the pyroxenite as an effect of more fertile bulk composition, the pressure shift of Stage 2 is not easily explainable. FACE geobarometer was calibrated for peridotite bulks having a narrow range of Na_2O/CaO and X_{Cr} ratios (Fig. 2). Olivine-bearing websterites may have bulk composition significantly different from the peridotite range and this potentially introduces a deviation in the FACE

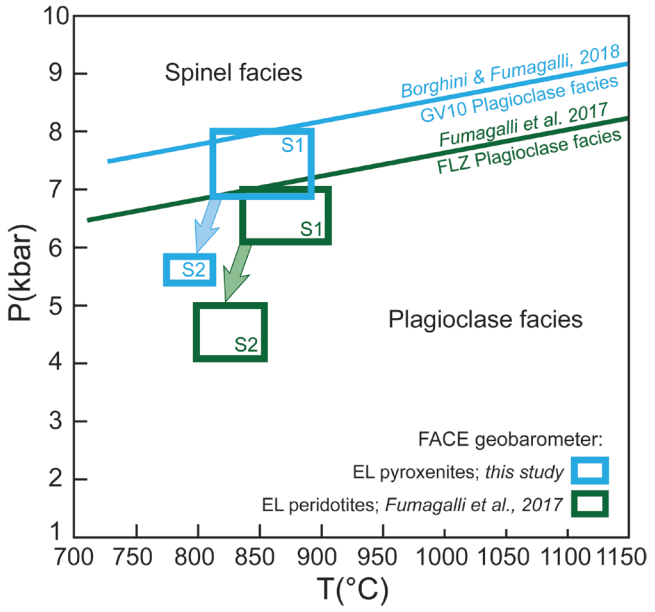

Fig. 7 - Geothermobarometric estimates for the peridotite and pyroxenite samples represented in a Pressure-Temperature diagram. Plagioclase-out boundaries for FLZ and GV10 bulk compositions were determined experimentally by Fumagalli et al. (2017) and Borghini and Fumagalli (2018). Stage S1 corresponds to the partial plagioclase-facies recrystallization provided by the cores of the neoblastic minerals (onset of recrystallization) and stage S2 corresponds to the subsequent shallower equilibration indicated by the compositions of the neoblastic rims

pressure estimates. Equilibrium temperatures yielded by pyroxenites are similar, or very close, to those estimated for peridotite; anyway, temperature has a minor effect on pressures computed by FACE geobarometer (Fumagalli et al., 2017).

This deviation might be considered looking at the activities used to calculate the Kd of the reaction Forsterite^{Ol} + Anorthite^{Pl} = Ca-Tschermak^{Cpx} + Enstatite^{Opx} (Table 2). In spite of different bulk Na_2O/CaO ratios, anorthite in plagioclase is not significantly different between the Suvero pyroxenites and peridotites (Fig. 5). This reflects the coherent Na-Ca partitioning between plagioclase and clinopyroxene in pyroxenites as well as in peridotites (Fig. 6b). The activity of enstatite in orthopyroxene (a_{en}) and of forsterite in olivine (a_{fo}) decreases concomitantly in agreement with the bulk X_{Mg} (Table 2). The discrepancy between the two compositional systems (pyroxenite vs. peridotite) is related to the variability of Ca-Tschermak activity in clinopyroxene ($a_{CaTs} = 4X_{Ca}X_{Al}{}^{M1}X_{Al}{}^{T}X_{Si}{}^{T}$). The latter is significantly higher in clinopyroxenes of pyroxenites resulting in higher pressure estimates provided by the FACE equation. Cr-Al partitioning between spinel and pyroxene is controlled by the spinel-pyroxene and clinopyroxene-orthopyroxene exchange reactions (Borghini et al., 2010):

$$\underset{\text{spinel}}{MgCr_2O_4} + \underset{\text{cpx}}{2CaAl_2SiO_6} = \underset{\text{spinel}}{MgAl_2O_4} + \underset{\text{cpx}}{2CaCrAlSiO_6} \quad (1)$$

$$\underset{\text{spinel}}{MgCr_2O_4} + \underset{\text{cpx}}{2MgAl_2SiO_6} = \underset{\text{spinel}}{MgAl_2O_4} + \underset{\text{cpx}}{2MgCrAlSiO_6} \quad (2)$$

$$\underset{\text{cpx}}{CaAl_2SiO_6} + \underset{\text{cpx}}{MgCrAlSiO_6} = \underset{\text{cpx}}{CaCrAlSiO_4} + \underset{\text{cpx}}{MgAl_2SiO_6} \quad (3)$$

At relatively low pressure, this partitioning is further complicated by the contribution of plagioclase according to the reaction:

$$\underset{\text{spinel}}{MgCr_2O_4} + \underset{\text{anorthite}}{CaAl_2Si_2O_8} = \underset{\text{opx}}{MgCrAlSiO_6} + \underset{\text{cpx}}{CaCrAlSiO_6} \quad (4)$$

As demonstrated by Borghini et al. (2010), X_{Cr} of spinel is positively correlated to the abundance of plagioclase, therefore, according to the continuous spinel-plagioclase reaction, at decreasing pressure the increase of X_{Cr} in spinel and pyroxenes is balanced by the modal plagioclase increase that is coupled to the decrease of spinel and pyroxene abundances. Hence, despite the role of spinel in incorporating Cr, pyroxenes represent important Chromium hosts even at low pressure (Borghini et al., 2010). For very low-X_{Cr} bulk compositions, as those of the pyroxenites studied here, the low Cr contents strongly limits these exchange reactions inhibiting the formation of Ca,Cr-Tschermak and Mg,Cr-Tschermak molecules in clinopyroxene and orthopyroxene, respectively. Therefore, at fixed P-T conditions and decreasing bulk X_{Cr}, the activity of Ca-Tschermak in equilibrium clinopyroxene is expected to increase. This is indeed shown by the negative correlation of the a_{CaTs} and X_{Cr} in clinopyroxene observed in Suvero peridotites and associated pyroxenites (Fig. 8). This could explain the deviation observed in pressure estimates computed for plagioclase-facies recrystallization stages by FACE geobarometer. However, experimental data on the mineral chemistry and element partitioning (e.g., Cr-Al partitioning between spinel and pyroxene) in low-pressure pyroxenite assemblages are so far very limited and more evidence of such deviation would need to be further investigated.

CONCLUDING REMARKS

Suvero pyroxenites show fine-grained neoblastic assemblages indicative of partial recrystallization at plagioclase-facies conditions. Core to rim chemical zonations in neoblastic mineral aggregates suggest equilibration stages at variable pressure and temperature. Combining microstructural observations and mineral chemistry, we identified two re-equilibration stages referring to the onset of plagioclase-facies re-crystallization ($T_{Fe\text{-}Mg}$ ~ 830-850°C, Stage 1) and a shallower colder re-equilibration ($T_{Fe\text{-}Mg}$ ~ 770-790°C, Stage 2). Application of FACE geobarometer provided equilibrium pressures ranging from 6.9 to 8.1±0.5 kbar for the Stage 1 and 5.8-5.9±0.5 kbar for the Stage 2. This decompressional evolution is consistent with exhumation history documented in the associated Suvero peridotite although at slightly higher equilibrium pressures. As the FACE geobarometer was calibrated for mantle peridotites, its application to pyroxenites, having significantly different bulk Na_2O/CaO and X_{Cr} compositions, may introduce a systematic deviation in pressure estimates. The variation of anorthite in plagioclase is rather similar in Suvero pyroxenites and peridotites. Remarkably, the much lower X_{Cr} in pyroxenites reflects in lower Cr incorporation in pyroxenes and, consequently, in significantly higher Ca-Tschermak activity in clinopyroxene. This might imply the systematic higher equilibrium pressure derived by FACE geobarometer.

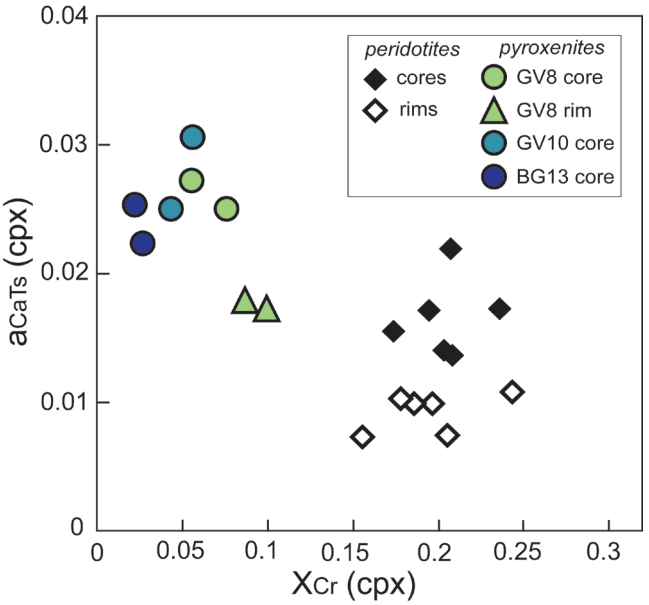

Fig. 8 - Activity of Ca-Tschermak vs. X_{Cr} (X_{Cr} = Cr/(Cr + Al_{VI}) in clinopyroxene from Suvero pyroxenites and peridotites. Data for peridotites are from Fumagalli et al. (2017). a_{CaTs} is calculated using the spread sheet provided by Fumagalli et al. (2017).

ACKNOWLEDGEMENTS

We thank R. Tilhac and C. Marchesi for constructive reviews of the manuscript, and A. Montanini for her work as editor. We also thank Paolo Campanella and Alessandra Gavoglio for realization of the thin section and Andrea Risplendente for assistance with the EPMA analyses. This research has been supported by the Italian Ministry of Education, University and Research (MIUR) through the grant [PRIN-2015C5LN35] "Melt-rock reaction and melt migration in the MORB mantle through combined natural and experimental studies".

Supplementary data to this article are available online at https://doi.org/10.4454/ofioliti.v45i1.529

REFERENCES

Basch V., Rampone E., Crispini L., Ferrando C., Ildefonse B. and Godard M., 2018. From mantle peridotites to hybrid troctolites: textural and chemical evolution during melt-rock interaction history (Mt. Maggiore, Corsica, France). Lithos, 323: 4-23, doi:10.1016/j.lithos.2018.02.025.

Basch V., Rampone E., Crispini L., Ferrando C., Ildefonse B. and Godard M., 2019a. Multi-stage reactive formation of troctolites in slow-spreading oceanic lithosphere (Erro-Tobbio, Italy): a combined field and petrochemical study. J. Petrol., 60: 873-906, doi: 10.1093/petrology/egz019.

Basch V., Rampone E., Borghini G., Ferrando C. and Zanetti A., 2019b. Origin of pyroxenites in the oceanic mantle and their implications on the reactive percolation of depleted melts. Contrib. Miner. Petrol., 174: 97, doi: 10.1007/s00410-019-1640-0.

Beccaluva L., Maciotta G., Piccardo G.B. and Zeda O., 1984. Petrology of lherzolitic rocks from the Northern Apennine ophiolites. Lithos, 17: 299-316, doi: 10.1016/0024-4937(84)90027-6.

Bodinier J.-L., Dupuy C. and Dostal J., 1988. Geochemistry and petrogenesis of Eastern Pyrenean peridotites. Geochim. Cosmochim. Acta, 52: 2893-2907, doi: 10.1016/0016-7037(88)90156-1.

Bodinier J.-L., Fabries J., Lorand J.-P., Dostal J. and Dupuy C., 1987a. Geochemistry of amphibole pyroxenite veins from the Lherz and Freychinede ultramafic bodies (Ariège, French Pyrénées). Bull. Minér., 110: 345-358.

Bodinier J.-L., Garrido C.J., Chanefo I., Bruguier O. and Gervilla F., 2008. Origin of pyroxenite-peridotite veined mantle by refertilization reactions: Evidence from the Ronda peridotite (Southern Spain). J. Petrol., 49: 999-1025, doi: 10.1093/petrology/egn014.

Bodinier J.-L., Guiraud M., Fabries J., Dostal J. and Dupuy C., 1987b. Petrogenesis of layered pyroxenites from the Lherz, Freychinède and Prades ultramafic bodies (Ariège, French Pyrénées). Geochim. Cosmochim. Acta, 51: 279-290, doi: 10.1016/0016-7037(87)90240-7.

Bonadiman C., Beccaluva L., Coltorti M. and Siena F., 2005. Kimberlite-like metasomatism and 'garnet signature' in spinel-peridotite xenoliths from Sal, Cape Verde archipelago: relics of a subcontinental mantle domain within the Atlantic oceanic lithosphere? J. Petrol., 46: 2465-2493, doi: 10.1093/petrology/egi061.

Borghini G. and Fumagalli P., 2018. Subsolidus phase relations in a mantle pyroxenite: an experimental study from 0.7 to 1.5 GPa. Eur. J. Mineral., 30 (2): 333-348, doi: 10.1127/ejm/2018/0030-2735.

Borghini G., Fumagalli P. and Rampone E., 2010. The stability of plagioclase in the upper mantle: subsolidus experiments on fertile and depleted lherzolite. J. Petrol., 51: 229-254, doi: 10.1093/petrology/egp079.

Borghini G., Fumagalli P. and Rampone E., 2011. The geobarometric significance of plagioclase in mantle peridotites: A link between nature and experiments. Lithos, 126: 42-53, doi: 10.1016/j.lithos.2011.05.012.

Borghini G., Fumagalli P. and Rampone E., 2017. Partial melting of secondary pyroxenite at 1 and 1.5 GPa, and its role in upwelling heterogeneous mantle. Contrib. Miner. Petrol., 172: 70, doi: 10.1007/s00410-017-1387-4.

Borghini G., Rampone E., Crispini L., De Ferrari R. and Godard M., 2007. Origin and emplacement of ultramafic-mafic intrusions in the Erro-Tobbio mantle peridotite (Ligurian Alps, Italy). Lithos, 94: 210-229, doi: 10.1016/j.lithos.2006.06.014.

Borghini G., Rampone E., Zanetti A., Class C., Cipriani A., Hofmann A.W. and Goldstein S.L., 2013. Meter-scale Nd isotopic heterogeneity in pyroxenite-bearing Ligurian peridotites encompasses global-scale upper mantle variability. Geology, 41: 1055-1058, doi: 10.1130/G34438.1.

Borghini G., Rampone E., Zanetti A., Class C., Cipriani A., Hofmann A.W. and Goldstein S.L., 2016. Pyroxenite layers in the Northern Apennines' upper mantle (Italy). Generation by pyroxenite melting and melt infiltration. J. Petrol., 57: 625-653, doi: 10.1093/petrology/egv074.

Borghini G., Rampone E., Zanetti A., Class C., Fumagalli P. and Godard M., 2019. Ligurian pyroxenite-peridotite sequences (Italy) and the role of melt-rock reaction in creating enriched-MORB mantle sources**.** Chem. Geol., in press, doi: 10.1016/j.chemgeo.2019.07.027, doi: 10.1016/j.chemgeo.2019.07.027.

Brey G.P. and Köhler T., 1990. Geothermobarometry in four phase lherzolites II. New thermobarometers, and practical assessment of existing thermobarometers. J. Petrol., 31: 1353-1378, doi: 10.1093/petrology/31.6.1353.

Dick H.J.B., Lissemberg C.J. and Warren J., 2010. Mantle melting, melt transport, and delivery beneath a slow-spreading ridge: the paleo-MAR from 23°15'N to 23°45'N. J. Petrol., 51: 425-467, doi: 10.1093/petrology/egp088.

Frey F.A., Shimizu N., Leinbach A., Obata M. and Takazawa E., 1991. Compositional variations within the Lower Layered Zone of the Horoman peridotite, Hokkaido, Japan: Constraints on models for melt-solid segregation. In: M.A. Menzies et al. (Eds.), Orogenic lherzolite and mantle processes. J. Petrol., 2: 211-227, doi: 10.1093/petrology/Special_Volume.2.211.

Fumagalli P., Borghini G., Rampone E. and Poli S., 2017. Experimental calibration of Forsterite-Anorthite-Ca**-**Tschermak-Enstatite (FACE) geobarometer for mantle peridotites. Contrib. Miner. Petrol., 172: 38, doi: 10.1007/s00410-017-1352-2.

Garrido C.J. and Bodinier J.-L., 1999. Diversity of mafic rocks in the Ronda peridotite: evidence for pervasive melt-rock reaction during heating of subcontinental lithosphere by upwelling asthenosphere. J. Petrol., 40: 729-754, doi: 10.1093/petroj/40.5.729.

Green D.H. and Falloon T.J., 1998. Pyrolite: a Ringwood concept and its current expression. In I. Jackson (Ed.), The Earth's mantle, Cambridge Univ. Press, Cambridge, p. 311-378, doi: 10.1017/CBO9780511573101.010.

Gysi A.P., Jagoutz O., Schmidt M.W. and Targuisti K., 2011. Petrogenesis of pyroxenites and melt infiltrations in the ultramafic complex of Beni Bousera, Northern Morocco. J. Petrol., 52: 1676-1735, doi: 10.1093/petrology/egr026.

Hidas K., Garrido C.J., Tommasi A., Padròn-Navarta J.A., Thielmann M., Konc Z., Frets E. and Marchesi C., 2013. Strain localization in pyroxenite by reaction-enhanced softening in the shallow subcontinental lithospheric mantle. J. Petrol., 54: 1997-2031, doi: 10.1093/petrology/egt039.

Ionov D.A., O'Reilly S.Y. and Ashchepkov V., 1995. Feldspar-bearing lherzolite xenoliths in alkali basalts from Hamar-Daban Baikal region, Russia. Contrib. Miner. Petrol., 122: 174-190, doi: 10.1007/s004100050120.

Kaczmarek M.A. and Müntener O., 2010. The variability of peridotite composition across a mantle shear zone (Lanzo massif, Italy): interplay of melt focusing and deformation. Contrib. Miner. Petrol., 160: 663-679, doi: 10.1007/s00410-010-0500-8.

Kelemen P.B., Kikawa E. and Miller D.J., 2007. Leg 209 summary: processes in a 20-km-thick conductive boundary layer beneath the Mid-Atlantic Ridge, 14°-16°N. In: P.B. Kelemen, E. Kikawa and D.J. Miller (Eds.), Proceed. ODP, Sci. Res., 209: 1-33, doi: 10.2973/odp.proc.sr.209.001.2007.

Kumar N., Reisberg L. and Zindler A., 1996. A major and trace element and strontium, neodymium, and osmium isotopic study of a thick pyroxenite layer from the Beni Bousera ultramafic complex of northern Morocco. Geochim. Cosmochim. Acta, 60: 1429-1444, doi: 10.1016/0016-7037(95)00443-2.

Le Roux V., Bodinier J.-L., Tommasi A., Alard O., Dautria J.M., Vauchez A. and Riches A.J.V., 2007. The Lherz spinel lherzolite: refertilized rather than pristine mantle. Earth Planet. Sci. Lett., 259: 599-612, doi: 10.1016/j.epsl.2007.05.026.

MacLeod C.J., Searle S.C., Murton B.J., Casey J.F., Mallows C., Unsworth S.C. and Achenbach K.L., 2009. Life cycle of oceanic core complexes. Earth Planet. Sci. Lett., 287: 333-344, doi: 10.1016/j.epsl.2009.08.016.

Manatschal G. and Müntener O., 2009. A type sequence across an ancient magma-poor ocean-continent transition: the example of the western Alpine Tethys ophiolites. Tectonophysics, 473: 4-19, doi: 10.1016/j.tecto.2008.07.021.

Marroni M., Molli G., Montanini A. and Tribuzio R., 1998. The association of continental crust rocks with ophiolites in the Northern Apennines (Italy): implications for the continent-ocean transition in the Western Tethys. Tectonophysics, 292: 43-66, doi: 10.1016/S0040-1951(98)00060-2.

Martin A.P., Cooper A.F. and Price R.C., 2014. Increased mantle heat flow with on-going rifting of the West Antarctic rift system inferred from characterisation of plagioclase peridotite in the shallow Antarctic mantle. Lithos, 190-191: 173-190, doi: 10.1016/j.lithos.2013.12.012.

Montanini A. and Tribuzio R., 2015. Evolution of recycled crust within the mantle: constraints from the garnet pyroxenites of the External Ligurian ophiolites (Northern Apennines, Italy). Geology, 43: 911-914, doi: 10.1130/G36877.1.

Montanini A., Tribuzio R. and Anczkiewicz R., 2006. Exhumation history of a garnet pyroxenite-bearing mantle section from a continent ocean transition (Northern Apennine ophiolites, Italy). J. Petrol., 47: 1943-1971, doi: 10.1093/petrology/egl032.

Montanini A., Tribuzio R. and Thirlwall M., 2012. Garnet clinopyroxenite layers from the mantle sequences of the Northern Apennine ophiolites (Italy): Evidence for recycling of crustal material. Earth Planet. Sci. Lett., 351-352: 171-181, doi: 10.1016/j.epsl.2012.07.033.

Montanini A., Tribuzio R. and Vernia L., 2008. Petrogenesis of basalts and gabbros from an ancient continent-ocean transition (External Liguride ophiolites, Northern Italy). Lithos, 101: 453-479, doi: 10.1016/j.lithos.2007.09.007.

Morishita T. and Arai S., 2001. Petrogenesis of corundum-bearing mafic rock in the Horoman Peridotite Complex, Japan. J. Petrol., 42: 1279-1299, doi: 10.1093/petrology/42.7.1279.

Mukasa S.B. and Shervais J.W., 1999. Growth of sub-continental lithosphere: Evidence from repeated injections in the Balmuccia lherzolite massif, Italian Alps. Lithos, 48: 287-316, doi: 10.1016/S0419-0254(99)80016-0.

Müntener O., Pettke T., Desmurs L., Meier M. and Schaltegger R., 2004. Refertilization of mantle peridotite in embryonic ocean basins: trace element and Nd isotopic evidence and implications for crust-mantle relationships. Earth Planet. Sci. Lett., 221: 293-308, doi: 10.1016/S0012-821X(04)00073-1.

Niu Y.L., 2004. Bulk-rock major and trace element compositions of abyssal peridotites: implications for mantle melting, melt extraction and post-melting processes beneath mid-ocean ridges. J. Petrol., 45: 2423-2458, doi: 10.1093/petrology/egh068.

Pearson D.G., Davies G.R. and Nixon P.H., 1993. Geochemical constraints on the petrogenesis of diamond facies pyroxenites from the Beni Bousera peridotite massif, North Morocco. J. Petrol., 34: 125-172, doi: 10.1093/petrology/34.1.125.

Piccardo G.B., Messiga B. and Vannucci R., 1988. The Zabargad peridotite-pyroxenite association: petrological constraints on its evolution. Tectonophysics, 150: 135-162, doi: 10.1016/0040-1951(88)90299-5.

Piccardo G.B., Rampone E. and Romairone A., 2002. Formation and composition of the oceanic lithosphere of the Ligurian Tethys: inferences from the Ligurian ophiolites. Ofioliti, 27: 145-161.

Piccardo G.B., Rampone E., Vannucci R., Shimizu N., Ottolini L. and Bottazzi P., 1993. Mantle processes in the sub-continental lithosphere: the case study of the rifted spinel-lherzolites from Zabargad (Red Sea). Eur. J. Miner., 5 (6): 1039-1056. https://doi.org/10.1127/ejm/5/6/1039.

Piccardo G.B., Zanetti A. and Müntener O., 2007. Melt-peridotite interaction in the southern Lanzo peridotite: field, textural and geochemical evidence. Lithos, 94: 181-209, doi: 10.1016/j.lithos.2006.07.002.

Rampone E. and Piccardo G.B., 2000. The ophiolite-oceanic lithosphere analogue: new insights from the Northern Apennine (Italy). In: J. Dilek, E. Moores, D. Elthon and A. Nicolas, (Eds.), Ophiolites and oceanic crust: New insights from field studies and Ocean Drilling Program, vol. 49. Geol. Soc. Am. Spec. Pap., p. 21-34, doi: 10.1130/0-8137-2349-3.21.

Rampone E., Borghini G. and Basch V., 2018. Melt migration and melt-rock reaction in the Alpine-Apennine peridotites: insights on mantle dynamics in extending lithosphere. Geosci. Front., in press, doi: 10.1016/j.gsf.2018.11.001.

Rampone E., Borghini G., Godard M., Ildefonse B., Crispini L. and Fumagalli P., 2016. Melt/rock reaction at oceanic peridotite/gabbro transition as revealed by trace element chemistry of olivine. Geochim. Cosmochim. Acta, 190: 308-331, doi: 10.1016/j.gca.2016.06.029.

Rampone E., Hofmann A.W., Piccardo G.B., Vannucci R., Bottazzi P. and Ottolini L., 1995. Petrology, mineral and isotope geochemistry of the External Liguride peridotites (Northern Apennines, Italy). J. Petrol., 123: 61-76, doi: 10.1093/petrology/36.1.81.

Rampone E., Hofmann A.W., Piccardo G.B., Vannucci R., Bottazzi P. and Ottolini L., 1996. Trace element and isotope geochemistry of depleted peridotites from an N-MORB type ophiolite (Internal Liguride, N. Italy). Contrib. Miner. Petrol., 123: 61-76, doi: 10.1007/s004100050143.

Rampone E., Piccardo G.B. and Hofmann A.W., 2008. Multistage melt-rock interaction in the Mt. Maggiore (Corsica, France) ophiolitic peridotites: microstructural and geochemical records. Contrib. Miner. Petrol., 156: 453-475, doi: 10.1007/s00410-008-0296-y.

Rampone E., Piccardo G.B., Vannucci R. and Bottazzi P., 1997. Chemistry and origin of trapped melts in ophiolitic peridotites. Geochim. Cosmochim. Acta, 61: 4557-4569, doi: 10.1016/S0016-7037(97)00260-3.

Rampone E., Piccardo G.B., Vannucci R., Bottazzi P. and Ottolini L., 1993. Subsolidus reactions monitored by trace element partitioning: the spinel- to plagioclase-facies transition in mantle peridotites. Contrib. Miner. Petrol., 115: 1-17, doi: 10.1007/BF00712974.

Rampone E., Romairone A., Abouchami W., Piccardo G.B. and Hofmann W., 2005. Chronology, petrology and isotope geochemistry of the Erro-Tobbio peridotites (Ligurian Alps, Italy): records of late Palaeozoic lithospheric extension. J. Petrol., 46: 799-827, doi: 10.1093/petrology/egi001.

Rampone E., Romairone A. and Hofmann A.W., 2004. Contrasting bulk and mineral chemistry in depleted peridotites: evidence for reactive porous flow. Earth Planet. Sci. Lett., 218: 491-506, doi: 10.1016/S0012-821X(03)00679-4.

Sano S. and Kimura J.I., 2007. Clinopyroxene REE geochemistry of the Red Hills peridotite, New Zealand: interpretation of magmatic processes in the upper mantle and in the Moho transition zone. J. Petrol., 48: 113-139, doi: 10.1093/petrology/egl056.

Sinigoi S., Comin-Chiaramonti P. and Alberti A.A., 1980. Phase relations in the partial melting of the Baldissero spinel-lherzolite (Ivrea-Verbano Zone, Western Alps, Italy). Contrib. Miner. Petrol., 75: 111-121, doi: 10.1007/BF00389772.

Sinigoi S., Comin-Chiaramonti P., Demarchi G. and Siena F., 1983. Differentiation of partial melts in the mantle: evidence from the Balmuccia peridotite, Italy. Contrib. Miner. Petrol., 82: 351-359, doi: 10.1007/BF00399712.

Suen C.J. and Frey F.A., 1987. Origin of the mafic and ultramafic rocks in the Ronda peridotite. Earth Planet. Sci. Lett., 85: 183-202, doi: 10.1016/0012-821X(87)90031-8.

Takazawa E., Frey F.A., Shimizu N., Saal N. and Obata M., 1999. Polybaric petrogenesis of mafic layers in the Horoman peridotite complex, Japan. J. Petrol., 40: 1827-1831, doi: 10.1093/petroj/40.12.1827.

Takazawa E., Frey F.A., Shimizu N. and Obata M., 2000. Bulk rock compositional variations in an upper mantle peridotite (Horoman, Hokkaido, Japan): are they consistent with a partial melting process? Geochim. Cosmochim. Acta, 64: 695-716, doi: 10.1016/S0016-7037(99)00346-4.

Taylor W.R., 1998. An experimental test of some geothermometer and geobarometer formulations for upper mantle peridotites with application to the thermobarometry of fertile lherzolite and garnet websterite. N. Jahrb. Miner., Abhandl., 172: 381-408.

Tribuzio R., Thirlwall M.F. and Vannucci R., 2004. Origin of the gabbro-peridotite association from the Northern Apennine ophiolites (Italy). J. Petrol., 45: 1109-1124, doi: 10.1093/petrology/egh006.

Van der Wal D. and Vissers R.L.M., 1996. Structural petrology of the Ronda peridotite, SW Spain: deformation history. J. Petrol., 37: 23-43, doi: 10.1093/petrology/37.1.23.

Voshage H., Sinigoi S., Mazzucchelli M., Demarchi G., Rivalenti G. and Hofmann A.W., 1988. Isotopic constraints on the origin of ultramafic and mafic dikes in the Balmuccia peridotite (Ivrea Zone). Contrib. Miner. Petrol., 100: 261-267, doi: 10.1007/BF00379737.

Warren J.M., 2016. Global variations in abyssal peridotite compositions. Lithos, 248-251: 193-219, doi: 10.1016/j.lithos.2015.12.023.

Received, October 15, 2019
Accepted, November 23, 2019
First published online, November 24, 2019